

Impact of doping on the performance of p-type Be-doped Al_{0.29}Ga_{0.71}As Schottky diodes[☆]

Noorah A. Al-Ahmadi^{a,*}, Fadiyah A. Ebrahim^a, Hala A. Al-Jawhari^a, Riaz H. Mari^b,
Mohamed Henini^{c,d}

^a Department of Physics, King Abdulaziz University, Jeddah 21589, Saudi Arabia

^b Institute of Physics, University of Sindh, Jamshoro, Pakistan

^c School of Physics and Astronomy, University of Nottingham, NG7 2RD, UK

^d Nottingham Nanoscience and Nanotechnology Center (NNNC), University of Nottingham, NG7 2RD, UK

ARTICLE INFO

Keywords:

Schottky barrier height
Doping concentration effect
Current–voltage characteristics
Cheung's equation
Gaussian distribution of barrier heights

ABSTRACT

The effects of changing the acceptors concentration on the electrical characteristics of Au/Ti on Be-doped Al_{0.29}Ga_{0.71}As Schottky contact have been investigated in the temperature range of 100–400 K. Using three devices with three different doping levels, the barrier height (Φ_B), ideality factor (n) and series resistance (R_S) for each diode were evaluated using both thermionic emission (TE) theory and Cheung's method. Our experimental results showed that the sample with a moderate doping concentration of $3 \times 10^{16} \text{ cm}^{-3}$ has the best performance, including ideality factor of 1.25 and rectification ratio of 2.24×10^3 at room temperature. All samples showed an abnormal behavior of reducing Φ_B and increasing n with increase of temperature. This behavior was attributed, in case of low concentration samples, to barrier inhomogeneity and was explained by assuming a Gaussian distribution of barrier heights at the interface. While for the heavily doped sample, such non-ideal manner was ascribed with tunneling through the field emission (FE) mechanism.

1. Introduction

P-type Al_xGa_{1-x}As is one of the most commonly used material as an active layer in high mobility two-dimensional hole gases (2DHGs) heterostructures or as a window in PIN heterostructures due to its suitability for alpha particle detection [1,2]. Using beryllium (Be) as an acceptor dopant in Al_xGa_{1-x}As grown by molecular beam epitaxy (MBE), high hole concentrations as high as $\sim 10^{19} \text{ cm}^{-3}$, can easily be achieved with no surface morphological degradation [3,4]. Due to higher substitutional Be incorporation in (311)A GaAs plane, epitaxial layers deposited on a (311)A orientated GaAs substrates showed a greater efficiency than those deposited on (100) orientation. Photoluminescence and electrical measurements revealed that both optical properties [5] and hole mobilities of 2DHGs [6] in Be-doped Al_xGa_{1-x}As devices grown on (311)A plane were higher than those fabricated on (100) oriented samples. This enhancement of charge mobility and PL efficiency was attributed to a reduction of electrically active hole traps in (311)A epilayers as compared to those grown on (100) substrates [6]. Moreover, for the (311)A orientation, the number of traps was found to be inversely related

to dopant concentration. Specifically, five, two and one hole traps have been detected in samples doped with 1×10^{16} , 3×10^{16} and $1 \times 10^{17} \text{ cm}^{-3}$, respectively [7]. However, the actual impact of this variation in acceptors level on the device performance has not been reported. It is well known that the performance and reliability of these devices can be controlled by the Schottky barrier height (Φ_B) and the diode ideality factor (n), which both have a strong dependence on the doping concentration [8].

In this work we investigate the effect of varying the doping concentration on the performance and on the charge transport of three Be-doped Al_{0.29}Ga_{0.71}As Schottky diodes grown by molecular beam epitaxy (MBE) on (311)A GaAs substrates. The mechanism that governs the conduction for each of those diodes will be indicated at both low and high temperatures.

2. Experimental details

A set of three Al_xGaAs_{1-x} ($x = 0.29$) samples with different Be-doping concentrations grown by MBE on semi-insulating (311)A GaAs substrates have been studied. The samples are labelled D1, D2

Peer review under responsibility of the National University of Science and Technology MISIS.

^{*} Corresponding author.

E-mail address: nalahmadi@kau.edu.sa (N.A. Al-Ahmadi).

<http://dx.doi.org/10.1016/j.moem.2017.06.001>

Received 15 February 2017; Received in revised form 12 May 2017; Accepted 26 June 2017

2452-1779/ © 2017 The National University of Science and Technology MISIS. Production and hosting by Elsevier B.V. This is an open access article under the CC BY-NC-ND license (<http://creativecommons.org/licenses/by-nc-nd/4.0/>).

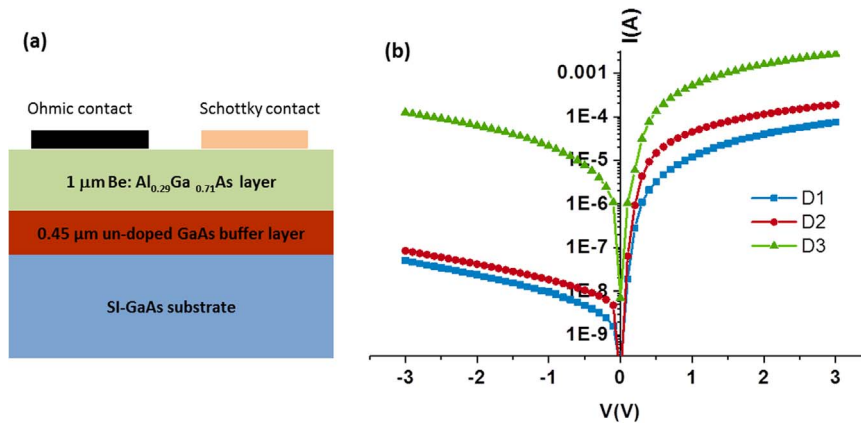


Fig. 1. (a) Schematic structure of the Be-doped $\text{Al}_{0.29}\text{Ga}_{0.71}\text{As}$ samples; (b) Room temperature I-V characteristics of three Schottky diodes with different doping concentrations; D1 = $1 \times 10^{16} \text{ cm}^{-3}$, D2 = $3 \times 10^{16} \text{ cm}^{-3}$ and D3 = $1 \times 10^{17} \text{ cm}^{-3}$.

Table 1
Forward to reverse current ratio (I_F/I_R) of the three diodes at room temperature.

| Sample ID | Doping concentration (cm^{-3}) | Rectifying ratio at RT. |
|-----------|---|-------------------------|
| D1 | 1×10^{16} | 1.48×10^3 |
| D2 | 3×10^{16} | 2.24×10^3 |
| D3 | 1×10^{17} | 22.4 |

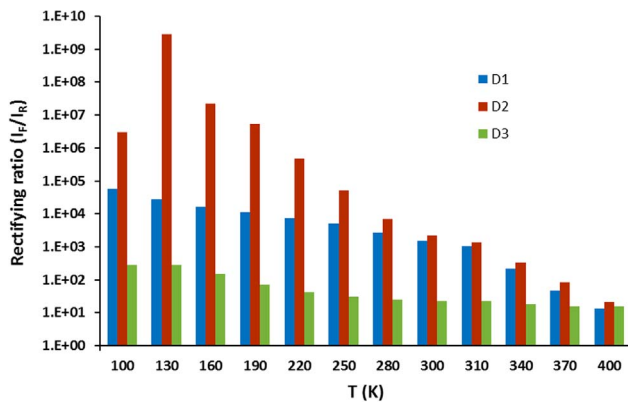


Fig. 2. Rectifying ratio of the three diodes D1, D2 and D3 at different temperatures.

and D3, and have doping concentrations of 1×10^{16} , 3×10^{16} and $1 \times 10^{17} \text{ cm}^{-3}$, respectively. The layer structure for all devices is similar as shown Fig. 1(a), and consists of 0.45 μm undoped GaAs buffer layer followed by Be-doped AlGaAs epitaxial layer with a thickness of 1 μm . Schottky contact with diameter 0.5mm was made by evaporating Ti/Au on the top of AlGaAs layer. A window on top layer has been etched for the deposition of ohmic contacts [Au/Ni/Au] which were then annealed at 360 $^\circ\text{C}$ in H_2/Ar mixture. The samples were mounted in a Janis CCS-450 helium closed loop cryostat whose temperature was controlled with a Lake Shore 331 S unit. The current-voltage (I-V) characteristics of the samples were measured using Keithley 238 source-measure unit (SMU) and a LabView software program. Different parameters were determined from I-V characteristics using a Matlab program.

3. Results and discussion

The rectifying behavior of the three diodes was compared based on their I-V characteristics at room temperature which are plotted in

Fig. 1(b). Rectifying ratio was calculated by dividing the forward current with the reverse current (I_F/I_R) at applied bias $V = \pm 1 \text{ V}$. The obtained values are listed in Table 1. Increasing the dopant concentration would result in more forward current according to the thermionic emission (TE) theory. However, the accompanying increase in the reverse current (leakage current) due to tunneling was found to be the main reason of degrading the diode rectification at high doping concentration. While the relative high reverse current for the device with lowest acceptors concentration D1 could be correlated to the existence of the interface states. It has been proved in a previous work [7] using deep level transient spectroscopy (DLTS) technique that sample D1 has the largest number of traps and interface defects. Therefore, the device with a moderate doping concentration of $3 \times 10^{16} \text{ cm}^{-3}$, D2, showed the higher rectification ratio at room temperature. In fact, we found that this diode showed the best rectifying behavior through the whole range of temperatures as it is illustrated in Fig. 2.

According to Padovani and Stratton [9], there are three types of current transport mechanisms through the Schottky barrier. Thermionic emission (TE) which occurs when the majority carriers have enough energy to overcome the barrier height, field emission (FE) which is a pure tunneling mechanism and thermionic field emission (TFE) assisted by interface states existing in the metal-semiconductor junction. While FE is a pure tunneling process, TFE is tunneling of thermally excited carriers which move through a thinner barrier. Therefore, TFE and FE mechanisms are function of carrier concentration, whereas, TE and TFE mechanisms are function of temperature [10].

In order to investigate the transport mechanism in each of Be-AlGaAs Schottky diodes, we plotted the I-V characteristics of the three diodes; D1, D2 and D3, on semi-logarithmic scale in the temperature range of 100–400 K as it is shown in Fig. 3(a-c). Noticeably, in all samples both forward and reverse currents increase with increasing temperature. However, the temperature dependence is more pronounced in the case of devices D1 and D2, which indicates that the charge transport mechanism in those diodes is controlled by the thermionic emission (TE) or thermionic-field emission (TFE).

Assuming a pure TE transport, I-V characteristics of the diodes can be analysed by the following relation [10];

$$I_D = I_S \exp \left[\left(\frac{qV - IR_S}{nkT} \right) \right] \quad (1)$$

where I_D is the current through the diode, I_S is the saturation current, V is the applied voltage, q is the electronic charge, R_S is the series resistance, T is the temperature in Kelvin, k is the Boltzmann constant, and n is the ideality factor. The saturation current I_S is given by [10],

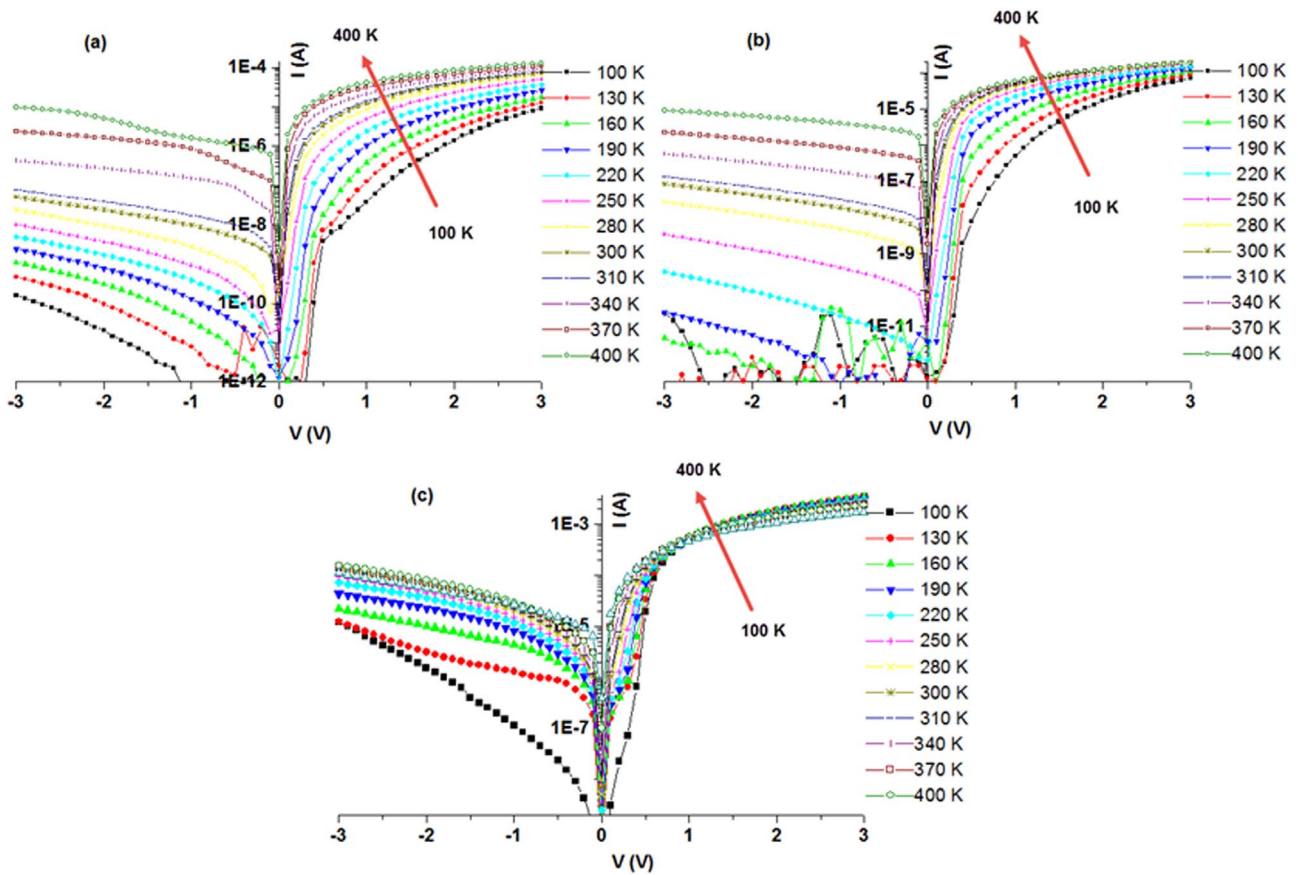


Fig. 3. Forward and reverse Current-Voltage (I-V) plots of Ti/Au/p-type AlGaAs Schottky diode at different temperatures with doping concentration of (a) $N_A=1 \times 10^{16} \text{cm}^{-3}$. (b) $N_A=3 \times 10^{16} \text{cm}^{-3}$. (c) $N_A=1 \times 10^{17} \text{cm}^{-3}$.

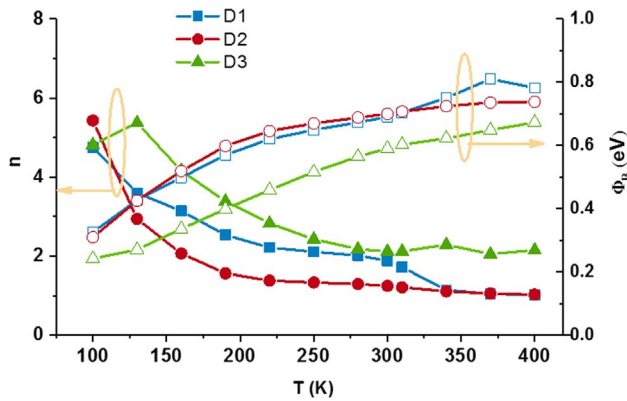


Fig. 4. Temperature dependence of ideality factor (represented by solid icons) and barrier height (represented by open icons) for various doping concentrations.

$$I_S = AA^*T^2 \exp\left(-\frac{q\Phi_B}{kT}\right) \quad (2)$$

Where Φ_B and A are the Schottky barrier height and the area of the diodes respectively. Rearranging the above equation gives us the following formula for determining the Schottky barrier height;

$$\Phi_B = \frac{kT}{q} \ln\left(\frac{AA^*T^2}{I_S}\right) \quad (3)$$

where A^* is the Richardson constant and it is equal to $9.48 \text{ A cm}^{-2} \text{ K}^{-2}$

for AlGaAs [11].

The ideality factor n , which is equal to unity in TE theory, is a measure of the fitting of the diode to the ideal TE theory. This significant factor can be extracted from the slope of the linear region of the forward bias $\ln(I)$ - V curves at low voltages according to [10];

$$n = \frac{q(V_2 - V_1)}{kT \ln(I_2/I_1)} \quad (4)$$

The varying of barrier height and ideality factor with temperature for diodes D1, D2 and D3, in the temperature range of 100–400 K, is shown in Fig. 4.

For all doping concentrations, the effective barrier height Φ_B increase by increasing temperature. The values of Φ_B for D1, D2 and D3 varied from 0.325, 0.309 and 0.242 eV at 100 K to 0.689, 0.699 and 0.590 eV at 300 K, respectively. On the other hand, Φ_B found to decrease with increasing the doping concentration. In general, the obtained values of Φ_B in those p-type Schottky diodes are lower than those reported for Ti/n-type AlGaAs barrier height with similar doping concentration [12].

According to TE model the ideality factor of a diode should be close to unity. However, D1 and D3 showed a deviation from unity, specifically at low temperatures, indicating the involving of other mechanism. Conversely, the diode D2 showed values that fulfilled with the TE model down to 210 K, after which n started to increase gradually. It well known that at lower temperatures, the carriers do not have sufficient energy to overcome the high barrier. The dominant current mechanism in this case would be through the patches of lower Schottky barrier height, which causes the higher ideality factor [13]. Additionally, we noticed that n increases with increasing doping

Table 2

The series resistance, ideality factor and the theoretical barrier height using I-V analysis and Cheung's model for all devices at high temperatures.

| T(K) | R_S (k Ω) | | n | | Φ_B | |
|--|---------------------|-------------------|--------------|-------------------|--------------|-------------------|
| | I-V analysis | Cheung's equation | I-V analysis | Cheung's equation | I-V analysis | Cheung's equation |
| Sample D1 (Doping concentration 1×10^{16} cm$^{-3}$) | | | | | | |
| 280 | 69.01 | 65.04 | 2.016 | 2.527 | 0.672 | 0.639 |
| 300 | 52.97 | 50.06 | 1.881 | 2.421 | 0.690 | 0.655 |
| 310 | 47.94 | 44.96 | 1.720 | 2.320 | 0.703 | 0.664 |
| 340 | 36.05 | 34.16 | 1.146 | 1.829 | 0.750 | 0.690 |
| 370 | 24.23 | 25.02 | 1.045 | 1.593 | 0.809 | 0.712 |
| 400 | 20.43 | 19.28 | 1.020 | 1.818 | 0.782 | 0.738 |
| Sample D2 (Doping concentration 3×10^{16} cm$^{-3}$) | | | | | | |
| 280 | 16.36 | 15.55 | 1.295 | 1.823 | 0.688 | 0.624 |
| 300 | 15.52 | 14.71 | 1.248 | 1.844 | 0.699 | 0.635 |
| 310 | 15.28 | 14.44 | 1.212 | 1.852 | 0.707 | 0.641 |
| 340 | 14.91 | 13.99 | 1.112 | 1.890 | 0.724 | 0.659 |
| 370 | 14.82 | 13.86 | 1.053 | 1.912 | 0.736 | 0.683 |
| 400 | 14.78 | 13.92 | 1.028 | 1.836 | 0.738 | 0.711 |
| Sample D3 (Doping concentration 1×10^{17} cm$^{-3}$) | | | | | | |
| 280 | 1.126 | 1.077 | 2.177 | 2.565 | 0.565 | 0.540 |
| 300 | 1.118 | 1.089 | 2.116 | 2.374 | 0.590 | 0.573 |
| 310 | 1.121 | 1.096 | 2.119 | 2.350 | 0.602 | 0.586 |
| 340 | 1.091 | 1.067 | 2.287 | 2.477 | 0.622 | 0.611 |
| 370 | 1.338 | 1.289 | 2.051 | 2.361 | 0.648 | 0.636 |
| 400 | 1.562 | 1.498 | 2.149 | 2.274 | 0.673 | 0.669 |

concentration, as it ranges from 1.88 and 1.24 for D1 and D2 at T = 300 K to 2.117 for D3 which is the heavily doped sample, these values makes D2, the diode with a moderate doping concentration, more ideal compared to the other diodes.

The barrier height Φ_B and other Schottky diode parameters such as the ideality factor n and the series resistance R_S were estimated using Cheung's equations which can be summarized as [14];

$$\frac{dV}{d(\ln I)} = IR_S + n \left(\frac{kT}{q} \right) \quad (5)$$

and

$$H(I) = IR_S + n\Phi_B \quad (6)$$

The experimental diode parameters given by Cheung's functions $dV/d(\ln I)$ and $H(I)$ are calculated at different temperatures and doping concentrations of Be-doped AlGaAs and the extracted barrier height Φ_B , ideality factor (n) and series resistance (R_S) are given in Table 2. By decreasing the temperature the R_S values increase and in turn, the ideality factors of all diodes become higher than unity. Thus, due to the series resistance, I-V characteristics of the diodes exhibit a non-linear behavior at low temperatures. The function $H(I)$ versus current in Eq. (6) should give a straight line in the forward bias I-V characteristics to determine R_S and barrier height Φ_B values. We found that our experimental data are much fitting to Cheung's equation at higher temperatures, as a non-linear line obtained when we tried to fit our low temperature readings.

The values of the barrier heights Φ_B of the diodes at different temperatures and doping concentrations as calculated using Eq. (3) and Cheung's Eq. (6) are given in Table 2. A good agreement between the values estimated by the two methods was obtained. But since parameters based on Cheung's method were calculated only at high temperatures (280–400 K), the comparison was limited within this range.

It can be noticed from Table 2 that the series resistance R_S is temperature dependent for D1 and D2 as it decreases with increasing temperature. However, the change is less clear in the sample D3 with

high doping concentration (1×10^{17} cm $^{-3}$). Such observation supports the assumption that D3 is governing by FE process which is temperature independent.

The increase in the barrier height and the decrease in the ideality factor with the increase in the temperatures points to a divergence from the pure TE theory. This behaviour which is inconsistent with TE theory could be explained by considering either a tunneling process, such as TFE or FE, through the Schottky junction [10] or the inhomogeneity of barrier height [15]. If current transport is controlled by TFE theory, tunneling will contribute to the diode current and Eq. (1) is no longer valid. The relation between the forward current and voltage in this case is given by [9],

$$I = I_0 \left[\exp \left(\frac{qV}{n_i kT} \right) \right] \quad (7)$$

with

$$n_i = \frac{qE_{00}}{kT} \coth \left(\frac{E_{00}}{kT} \right) \quad (8)$$

where E_{00} is the characteristic tunneling energy, which is related to the transmission probability of the carrier through the barrier and it is given by [16]:

$$E_{00} = \frac{q\hbar}{2} \sqrt{\frac{N_A}{m_h^* \epsilon_s}} \quad (9)$$

where \hbar is Planck's constant, ϵ_s is the semiconductor dielectric constant and m_h^* is the hole effective mass. This parameter provides a good assessment to clarify whether the dominating mechanism is TE or TFE. For $E_{00} \ll kT$, there is no existence of tunneling through the barrier height and the TE is the dominant mechanism. When $E_{00} \approx kT$, the carrier transport mechanism known as TFE and FE should be valid when $E_{00} \gg kT$ [17]. In the case of p-type Be:AlGaAs Schottky diode with doping concentrations of 1×10^{16} , 3×10^{16} and 1×10^{17} cm $^{-3}$, the theoretical values of E_{00} are found to be about 0.7, 1.21 and 2.21 meV respectively using $m_h^* = 0.58m_0$ and $\epsilon_s = 12.08$ [18]. According to these small calculated values of E_{00} , the conduction

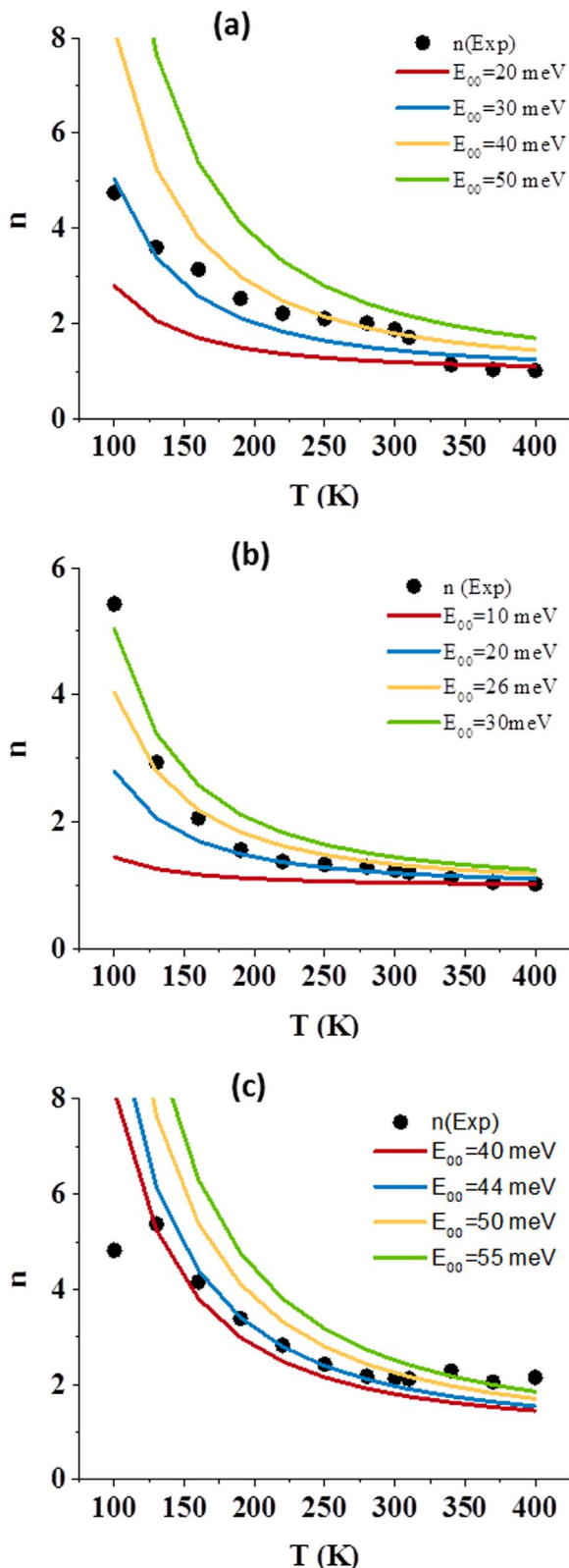


Fig. 5. Temperature dependence of tunneling ideality factor according to Eq. (8), at different values of E_{00} . Closed circles indicate the temperature dependence of ideality factor values obtained experimentally from (I-V) characteristics for (a) D1, (b) D2 and (c) D3.

mechanism at all temperatures should be governed by TE. However, experimentally the values of E_{00} are usually much higher due to the enhancement of electric field on the semiconductor surface [19] or the

increase of density of states at MS interface [20]. Any of these changes could affect the apparent E_{00} values and hence the current mechanism. To find the experimental values of E_{00} , we plotted the relation between n_t (tunneling ideality factor as determined from Eq. (8)) and T at different proposed values of E_{00} as they are illustrated by solid lines in Fig. 5(a-c). The filled circles in Fig. 5(a-c) represent the values of ideality factor calculated experimentally from I-V curves for D1, D2 and D3, respectively.

The E_{00} values obtained by matching the experimental readings of n (I-V) with the theoretical values of n_t for all samples are listed in Table 3. Comparing the values of E_{00} with the carriers' thermal energy (kT) allows us to predict the mechanism of current transport at each range of temperature. It is clear that the tunneling parameter of the heavily doped sample, D3, is larger than kT at the whole range of temperature. This fact proves that FE is the predominant current transport mechanism in D3 and for this reason, the non-ideal behavior of the ideality factor and the barrier height with temperature is detected. On the other hand, E_{00} obtained from samples with lighter doping, D1 and D2, showed that TE is the main current transport mechanism in those samples except at low temperatures where the leakage through barrier patches become more pronounced. Consequently, the abnormal behavior noticed in D1 and D2 with rise in temperature cannot be attributed to tunneling but rather to the barrier height inhomogeneities [9]. The combination of low and high barrier patches with individual cross sectional areas at the interface between metal and semiconductor may result in enhancement of the electric field which, in hence, reduces the barrier height [21]. The inhomogeneous Schottky barrier could be explained by means of Gaussian distribution with a standard deviation σ_0 around a mean barrier height Φ_{b0} value that is expressed by [22];

$$\Phi_{bo} = \Phi_{b0(\text{mean})} - \frac{q\sigma_0^2}{2kT} \quad (10)$$

The value of σ_0 is considered as a measure of the barrier inhomogeneity. The lower the σ_0 is, the more ideal the performance of the diode will be [23].

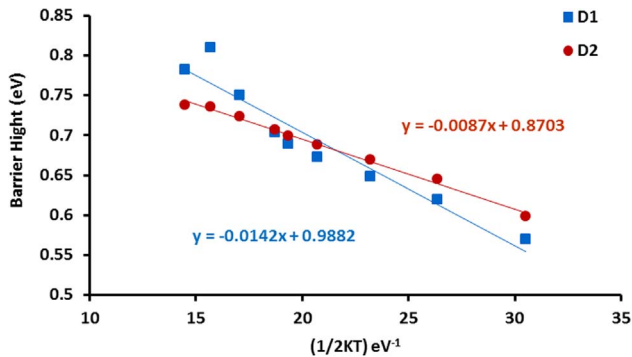
From the intercept and slope of a linear fit to a plot of Φ_{b0} versus $1/2kT$ (Fig. 6), $\Phi_{b0(\text{mean})}$ and σ_0 are extracted to be 0.988 and 0.142 eV, for D1 and 0.870 and 0.087 eV, for D2, respectively. The calculated values of σ_0 for both diodes are significant compared to Φ_{b0} , which implies the existence of 12.1% and 10.7% of barrier inhomogeneity in Schottky diodes D1 and D2, respectively. These results show that the temperature dependent experimental data of the Schottky diodes D1 and D2 are in agreement with the model which is related to thermionic emission over a Gaussian barrier height distribution [22,24,25].

4. Conclusions

I-V characteristics and transport mechanisms of Au/Ti/p-Al_{0.29}Ga_{0.71}As Schottky junction with different doping concentrations have been investigated in the temperature range of 100–400 K. The basic diode parameters such as barrier height, ideality factor and series resistance are extracted using thermionic emission TE theory and Cheung's method. Based on the estimated value of the characteristic energy E_{00} , field emission process found to be the main transport mechanisms in sample D3 with high doping concentration. However, at lower concentrations we believe that current transport is governed by thermionic emission over a Gaussian barrier height distribution. Through all temperatures range, the sample with moderate doping concentration ($3 \times 10^{16} \text{ cm}^{-3}$) showed the best performance with more stability in ideality factor.

Table 3Extracted values of E_{00} for the three Schottky diodes through the temperature range of 100–400 K.

| Diode | D1 | | D2 | | D3 | |
|---------------------------|--------------------|---------|--------------------|---------|--------------------|---------|
| N_A (cm ⁻³) | 1×10^{16} | | 3×10^{16} | | 1×10^{17} | |
| T(K) | 100–310 | 340–400 | 100–220 | 250–400 | 100–310 | 340–400 |
| E_{00} (me V) | 30–40 | 20 | 30–20 | 20–10 | 40–44 | 55 |
| kT (me V) | 8–27 | 29–35 | 8–19 | 22–34 | 8–26 | 29–34 |
| Current mechanism | TFE | TE | TFE | TE | FE | |

**Fig. 6.** Plot of barrier height versus $1/2kT$ for D1 and D2.**References**

- [1] J. Szatkowski, K. Sieranski, E. Paczek-Popko, Z. Gumienny, Deep level defects in proton irradiated p-type $Al_{0.5}Ga_{0.5}As$, *Physica B* 404 (2009) 4967–4969.
- [2] V.A.Ka.V.V. Kozlovski, Doping of semiconductors using radiation defects produced by irradiation with protons and alpha particles, *Semiconductors* 35 (7) (2001) 735–761.
- [3] N. Galbiati, C. Gatti, E. Grilli, M. Guzzi, L. Pavesi, M. Henini, Photoluminescence determination of the be binding energy in direct-gap AlGaAs, *Appl. Phys. Lett.* 71 (21) (1997) 3120–3122.
- [4] S. Fujita, S.M. Bedair, M.A. Littlejohn, J.R. Hauser, Doping characteristics and electrical properties of Be-doped p-type $Al_xGa_{1-x}As$ by liquid phase epitaxy, *J. Appl. Phys.* 51 (10) (1980) 5438.
- [5] N. Galbiati, L. Pavesi, E. Grilli, M. Guzzi, M. Henini, Be doping of (311)A and (100) $Al_{0.24}Ga_{0.76}As$ grown by molecular beam epitaxy, *Appl. Phys. Lett.* 69 (27) (1996) 4215.
- [6] R. Mari, M. Shafi, M. Aziz, A. Khatab, D. Taylor, M. Henini, Electrical characterisation of deep level defects in Be-doped AlGaAs grown on (100) and (311)A GaAs substrates by MBE, *Nanoscale Res. Lett.* 6 (1) (2011) 1–5.
- [7] R.H. Mari, DLTS Characterisation of Defects in III–V Compound Semiconductors Grown by MBE, University of Nottingham, 2011.
- [8] S. Chand, P. Kaushal, J. Osvald, Numerical simulation study of current–voltage characteristics of a Schottky diode with inverse doped surface layer, *Mater. Sci. Semicond. Process.* 16 (2) (2013) 454–460.
- [9] F.A. Padovani, R. Stratton, Field and thermionic-field emission in Schottky barriers, *Solid-State Electron.* 9 (7) (1966) 695–707.
- [10] S.M. Sze, *Physics of Semiconductor Devices*, Wiley Sons, New York, 1981.
- [11] Y.H. Wang, M.P. Houng, F.H. Chen, P.W. Sze, Study of AuAgFe/AlGaAs Schottky diodes fabricated by in situ molecular beam epitaxy, *J. Mater. Sci.: Mater. Electron.* 3 (1992) 206–210.
- [12] N.A. Al-Ahmadi, H.A. Al-Jawhari, Effect of epitaxial layer thickness on the electrical properties of Ti/n-AlGaAs grown by MBE, *Results Phys.* 6 (2016) 67–69.
- [13] L. Huang, Barrier inhomogeneities of platinum contacts to 4H-SiC, *Superlattices Microstructures* 100 (2016) 648–655.
- [14] S.K. Cheung, N.W. Cheung, Extraction of Shottky diode parameters from forward current–voltage characteristics, *Appl. Phys. Lett.* 49 (1986) 2.
- [15] I. Jyothi, H.-D. Yang, K.-H. Shim, V. Janardhanam, S.-M. Kang, H. Hong, C.-J. Choi, Temperature dependency of Schottky barrier parameters of Ti Schottky contacts to Si-on-insulator, *Mater. Trans.* 54 (9) (2013) 1655–1660.
- [16] A.M. Rodrigues, Analysis of the current-transport mechanism across a CVD diamond/silicon interface, *Appl. Surf. Sci.* 253 (14) (2007) 5992–5999.
- [17] E.H. Rhoderick, R.H. Williams, *Metal-Semiconductor Contacts* 129, Clarendon Press, Oxford, 1988.
- [18] Energy Gap in III–V Ternary Semiconductors. Available from: (http://cleanroom.byu.edu/EW_ternary.phtml).
- [19] S.A. Yeriskin, M. Balbasi, S. Demirezen, Temperature and voltage dependence of barrier height and ideality factor in Au/0.07 graphene-doped PVA/n-Si structures, *Indian J Phys.* 91 (4) (2017) 421–430.
- [20] E. Ayyildiz, H. Cetin, Z.J. Horvath, Temperature dependent electrical characteristics of Sn/p-Si Schottky diodes, *Appl. Surf. Sci.* 252 (4) (2005) 1153–1158.
- [21] S.S. Naik, V.R. Reddy, Electrical transport characteristics and deep level transient spectroscopy of Ni/V/n-InP Schottky barrier diodes, *J. Nano Electron. Phys.* 4 (2) (2012) 02006.
- [22] J. Werner, aH. Güttler, Temperature dependence of Schottky barrier heights on silicon, *J. Appl. Phys.* 73 (1993) 3.
- [23] C.S. Guclu, A.F. Ozdemir, Ş. Altindal, Double exponential I-V characteristics and double Gaussian distribution of barrier heights in (Au/Ti)/ Al_2O_3 /n-GaAs (MIS) type Schottky barrier diodes in wide temperature range, *Appl. Phys. A* 122 (1032) (2016) 1–9.
- [24] S. Chand, A.J. Kumar, Effects of barrier height distribution on the behavior of a Schottky diode, *J. Appl. Phys.* 82 (1997) 10.
- [25] R. Singh, P. Sharma, M.A. Khan, V. Garg, V. Awasthi, A. Kranti, S. Mukherjee, Investigation of barrier inhomogeneities and interface state density in Au/MgZnO:Ga Schottky contact, *J. Phys. D: Appl. Phys.* 49 (44) (2016) 445303.